NASA TECHNICAL MEMORANDUM 104062
AVSCOM TECHNICAL REPORT 91-B-002

ANALYSIS OF MATRIX CRACKING AND LOCAL DELAMINATION IN $(0/\theta/-\theta)_s$ GRAPHITE EPOXY LAMINATES UNDER TENSION LOAD

S. A. Salpekar and T. K. O'Brien

March 1991

National Aeronautics and
Space Administration

Langley Research Center
Hampton, Virginia 23665

US ARMY
AVIATION
SYSTEMS COMMAND
AVIATION R&T ACTIVITY

ABSTRACT

Several 3-D finite element analyses of $(0/\theta/-\theta)_s$ graphite epoxy laminates, where θ=15, 20, 25, 30, and 45 degrees, subjected to axial tension load, were performed. The interlaminar stresses in the $\theta/-\theta$ interface were calculated with and without a matrix crack in the central $-\theta$ plies. The interlaminar normal stress changes from a small compressive stress when no matrix crack is present to a high tensile stress at the intersection of the matrix crack and the free edge. The analysis of local delamination from the $-\theta$ matrix crack indicates a high strain energy release rate and a localized mode I component near the free edge, within one ply distance from the matrix crack. In order to examine the stress state causing the matrix cracking, the maximum principal normal stress in a plane perpendicular to the fiber direction in the $-\theta$ ply was calculated in an uncracked laminate. The corresponding shear stress parallel to the fiber was also calculated. The principal normal stress at the laminate edge increases through the ply thickness and reached a very high tensile value at the $\theta/-\theta$ interface indicating that the crack in the $-\theta$ ply may initiate at the $\theta/-\theta$ interface. Crack profiles on the laminate edge in the $-\theta$ ply were constructed from the principal stress directions. The cracks were found to be more curved for layups with smaller θ angles, which is consistent with experimental observations in the literature.

1. INTRODUCTION

In laminated composite materials, matrix cracking and local delaminations from matrix cracks are important damage mechanisms which contribute to stiffness loss and eventual laminate failure [1,2]. Therefore, it is important to understand and predict the initiation and growth of this damage.

In the static tension test of a $[0_4/30_4/-30_4]_s$ graphite epoxy laminate, Soni and Kim [3] observed a curved crack in the -30 degree group of plies. The tests conducted on $[0_n/\pm 15]_s$ laminates by Lagace and Brewer [4] showed that the delamination area in the 15/-15 interface extended between the transverse ply crack and the free edge. O'Brien and Hooper [5] found that in $(0_2/\theta_2/-\theta_2)_s$ graphite epoxy laminates (θ=20, 25, 30 degrees) subjected to tension fatigue loading, matrix cracking was detected as the first event followed by local delamination. The matrix cracks formed near the stress-free edge and the local delaminations formed in the $\theta/-\theta$ interface. These local delaminations were bounded between the free edge and the matrix crack (figure 1). In an experimental and analytical study, Fish and O'Brien [6] concluded that in $(+15/90_n/-15)_s$ glass epoxy laminates the interlaminar tensile stresses due to cracking in the +15 degree ply plays a significant role in the onset of local delaminations.

The purpose of this paper is to study the stress state causing matrix cracking and delamination in the $(0/\theta/-\theta)_s$ graphite epoxy laminates subjected to axial tension. Three dimensional finite element analyses were performed on $(0/\theta/-\theta)_s$ laminates for θ=15, 20, 25, 30, and 45 degrees. The effect of the

$-\theta$ degree ply crack on the interlaminar stress in the $\theta/-\theta$ interface was evaluated. A strain energy release rate analysis of delamination from the $-\theta$ ply crack was performed. In order to better understand the matrix cracking, the in-plane stresses in the $-\theta$ ply of the uncracked laminate were calculated. The principal stresses in the $-\theta$ ply were examined to predict the probable crack profile. The crack profiles predicted using the present analysis were compared with those from the experiments in the literature [5].

2. LAMINATE CONFIGURATION AND LOADING

A $(0/\theta/-\theta)_s$ graphite epoxy laminate subjected to axial tension load (figure 2) was analyzed using the finite element method. The laminate length was assumed to be 75h and the width was 10h, where h is the ply thickness. A unit ply thickness was assumed in the model. The Cartesian coordinate system has its origin at point A and the axes are shown in figure 2. The matrix crack was assumed to occur in the two $-\theta$ degree central plies, as evidenced in the experiments [5]. The direction of the matrix crack across the laminate width was assumed to be parallel to the fiber direction. For simplicity, the matrix crack was assumed to be straight through the thickness of the $-\theta$ ply and oriented normal to the XY plane. The laminate was assumed to be constrained at x=0 plane and an arbitrary uniform axial displacement of 0.5625h was applied on the x=75h face which corresponds to a strain of 0.0075.

The finite element discretization of the laminate used in the analysis is shown in figure 3. Only the top half of the laminate (above z=0) was modelled and appropriate symmetry boundary conditions were applied on the z=0 plane.

In order to analyze the effect of the stress free edge on matrix cracking and on local delamination, a finely graded mesh was used at one of the free edges (y=0). The smallest element size used in each direction was .01h and the mesh refinement is assumed to be adequate for stress analysis accuracy. The behavior of the matrix crack in the $(0/\theta/-\theta)_s$ laminate and the resulting local delaminations depend on the angle θ of the off-axis plies [5]. Therefore, the stress analysis was carried out for each of the laminates, where the angle θ was assumed to be 15, 20, 25, 30, and 45 degrees. A separate model was constructed for each case by assuming a matrix crack plane at the corresponding angle $-\theta$ (plane BCDE in figure 2) and a finely graded mesh was used on either side of the plane BCDE. The θ and $-\theta$ degree plies had six elements each through the thickness, and the mesh was finely graded near the $\theta/-\theta$ interface. A total of 4312, 20-node isoparametric tetrahedral elements having 20477 nodes were used in each model. The matrix crack and delamination were simulated by releasing coincident multi-point constraints provided in the model. The elastic constants for the graphite fiber and epoxy resin matrix material used in the analysis are shown in Table 1 [5].

3. ANALYSIS

Several 3-D finite element analyses were performed in order to study various aspects of matrix cracking and local delaminations initiating from the matrix cracks. The various analyses are described below.

3.1 INTERLAMINAR STRESSES: The $(0/15/-15)_s$ laminate was tested in reference 4 and the delamination was attributed to the interlaminar shear. Therefore the θ=15 degree case was analyzed here.

The experimental evidence [5] indicated that the local delamination on the $\theta/-\theta$ interface was associated with matrix cracking in the $-\theta$ degree ply. The crack in the -15 ply was assumed to be straight in the thickness direction, oriented normal to the XY plane, and parallel to the fiber direction. The interlaminar normal and shear stresses were obtained in the 15/-15 interface in the laminate before and after introducing a matrix crack in the -15 ply, to examine any change in these stresses due to the introduction of the matrix crack.

3.2 STRAIN ENERGY RELEASE RATE: Local delamination in the 45/-45 interface was modelled as initiating from a matrix crack in the -45 ply. The strain energy release rate (G) was calculated for small increments of delamination growth. The delamination front was assumed to be uniform and parallel to the matrix crack for convenience of modelling. The elements were in the shape of a parallelopiped, one side being parallel to the free edge. The virtual crack closure technique (VCCT) was used to compute the strain energy release rate [7]. The equations used in the G calculation are also given in Reference 8.

3.3 IN-PLANE STRESSES: The normal tension stress on the BCDE plane in an uncracked laminate was examined for θ=15, 30, and 45 degrees. If the tension stress extends only partially along the potential crack plane, then the matrix crack may extend only partially across the laminate width.

3.4 PRINCIPAL TENSION AND ACCOMPANYING SHEAR: The curved shape of the matrix crack on the stress free edge (y=0) in the $-\theta$ ply, observed in the experiments [5], may be due to the principal tension stress, rather than just the in-plane tension and in-plane shear stresses. The principal tension

stress may be acting at an angle other than 90 degrees to the vertical plane BCDE (figure 2). The principal tension stress acting perpendicular to the fiber was computed as explained below.

The 3-D finite element analysis of the intact laminate was performed using the appropriate mesh for the ply angle (θ) under consideration. The stresses at the nodes on the potential matrix crack surface BCDE (figure 2) were then transformed to the coordinate system 123 (figure 4) on plane FGHJ which is normal to plane BCDE. In the system 123, axis 1 was normal to the vertical plane BCDE, axis 2 was parallel to BCDE and the axis 3 was vertical (parallel to z direction). The principal normal stress due to the three stress components (σ_{11}, σ_{33}, σ_{13}) in the 13 plane were computed at each node. The corresponding direction of the principal stress, i.e., the angle α measured counter-clockwise from axis 1, was also determined at each node. The six stress components in the 123 coordinate system were then transformed through the angle α in the 1'3' plane so that axis 1' coincides with the principal direction.

The new coordinate system 1'2'3' is also shown in figure 4. The purpose of this second transformation was twofold. The normal stress $\sigma_{1'1'}$, on the transformed plane in the 1' direction should check with the principal stress calculated earlier. In addition, the shear stress acting parallel to the fiber direction on this plane ($\tau_{1'2'}$) was obtained. Thus, the principal tension stress normal to the fiber direction, the angle α indicating the direction of the principal stress in the 1'2' plane, and the shear stress acting parallel to the fiber direction were obtained for each node on plane

BCDE. This analysis was repeated for the five types of laminates, with ply angles, θ, of 15, 20, 25, 30, and 45 degrees.

4. RESULTS AND DISCUSSION

4.1 Interlaminar Stresses: The interlaminar normal stress, σ_z, in the +15/-15 interface, normalized by the remote applied axial stress, σ_o, was found to have a small compressive value near the free edge of the $(0/15/-15)_s$ uncracked laminate [5]. The 3D analysis of the laminate with a matrix crack in the -15 degree ply, however, indicated that there was a large tensile interlaminar normal stress at the intersection of the matrix crack and the stress free edge (fig. 5). This high interlaminar tension will contribute significantly to the onset of delamination in the 15/-15 interface (figure 1).

The interlaminar shear stress τ_{xz} in the +15/-15 interface of the uncracked laminate increases in magnitude towards the stress free edge but is uniform along any line parallel to the free edge. After modelling a crack in the -15 degree ply, the interlaminar shear stress increased in the area bounded by the matrix crack and the free edge (figure 6). The increase in interlaminar shear stress was less than one order of magnitude.

4.2 STRAIN ENERGY RELEASE RATE: A uniform delamination front growing parallel to a -45 degree ply crack in a $(0/45/-45)_s$ laminate was modelled. In this analysis, the direction of delamination growth is not normal to the delamination front and the delamination growth is modelled between dissimilar

materials. Therefore, this modelling was expected to give only a qualitative indication of the effect of the free edge on the strain energy release rate.

The variation of mode I component of G and the total G normalized by $\epsilon^2 t E_{11}$ with distance s along the delamination front, for a/h=0.02 are shown in figure 7. The symbols ϵ, t, and E_{11} denote the remote axial strain, the laminate thickness and Young's modulus in the fiber direction, respectively. Both the total G and G_I distributions show a marked increase within one ply thickness of the free edge. The Mode I component appears to be absent in the interior along the laminate width. Figure 8 shows the plots of normalized G versus a/h near the free edge of the laminate and in the interior of the laminate. G decreases as the delamination grows away from the matrix crack. Figure 8 also indicates that G is higher near the free edge than in the interior.

4.3 IN-PLANE STRESS: The plane BCDE parallel to the fiber direction shown in figure 2 is a potential crack plane in the $-\theta$ degree ply. The stress component normal to the plane BCDE was obtained for each point (node) on this plane. The points on plane BCDE where the normal stress changes from tension to compression are marked and joined to indicate the area under in-plane tension. The projection of plane BCDE and its area under tension, on yz plane is shown in figure 9, for laminates with θ=15, and 30 degrees. In order to obtain the area of plane BCDE under tension along the crack which is parallel to the fiber direction, the y coordinate must be increased by a factor of $1/\sin(\theta)$. Figure 9 shows that for θ=15, and 30 degrees the in-plane tension exists up to a distance of 1 to 1.5 plies in the y direction on yz projection or three to four plies in the $-\theta$ degree ply. This result is consistent with

the finding from quasi-3D analysis in ref.5. Furthermore, figure 9 shows that this in-plane tension extends through the thickness to the $\theta/-\theta$ interface only near the free edge. Therefore, the delamination may initiate between the θ and $-\theta$ plies where $-\theta$ ply meets the laminate edge. The in-plane normal stress for the $(0/45/-45)_s$ laminate, however, was tensile over the entire crack face. Hence, the matrix crack in the -45 ply and the delamination in the 45/-45 interface from -45 ply crack may extend further towards the interior of the laminate than for θ=15 - 30 degree cases.

4.4 MATRIX CRACK PROFILE: The angles (α) with respect to horizontal axis 1 (figure 4), at which the principal stress acts near the laminate edge were calculated for fiber angles 15,20,25,30, and 45 degrees. The values of α increase from the center of the laminate towards the $\theta/-\theta$ interface. Thus the plane on which the principal normal stress acts tends to move away from the vertical axis as z changes from 0 to 1. By using the values of α for various z coordinate values, it is possible to construct an approximate shape of the matrix crack caused by the principal normal tension stress $\sigma_{1'1'}$. The crack shapes constructed using this approach are shown in figure 10(a). The cracks appear to be curved towards the $\theta/-\theta$ interface. Figure 10(a) indicates that the crack shape for θ=45 degrees tends to be less curved than that for the smaller θ angles considered.

The crack profiles in figure 10(a) were constructed on FGHJ planes normal to the fiber direction (fig.2). In order to obtain the shape of the crack on the free edge, the crack must be projected using the corresponding fiber angle. This is achieved by multiplying the abscissa values in figure 10(a) by a factor of $(1/\sin\theta)$. The crack profiles on the free edge thus obtained are

shown in figure 10(b). Figure 10(b) clearly shows that as the angle θ decreases, the crack profile tends to be more curved. These analytical results exhibit the same trend as seen in the micrographs of the specimen edges from experiments on similar laminates [5], and are sketched in figure 11 for clarity.

During the course of the present analysis, the authors were made aware of the paper on the matrix cracking in cross-ply laminates by Groves et. al. [9]. Reference 9 also used the idea of principal stresses to address the occurrence of curved cracks in 90 degree plies and observed a similar correlation between the crack profile and direction of principal stress.

4.5 PRINCIPAL TENSION STRESS AND SHEAR STRESS: The values of the principal tension stress acting in a plane normal to the fiber direction at the free edge were calculated for fiber angles 15,20,25,30, and 45 degrees. The $\sigma_{1'1'}$ values increase from the laminate midplane (z=0) towards the $\theta/\text{-}\theta$ interface (z=1) for each of the laminates analyzed. The shear stress along the fiber direction, $\tau_{1'2'}$ increased from the laminate midplane towards the $\theta/\text{-}\theta$ interface, through the ply thickness for all values of θ as well.
The principal tensile stress and the shear stress calculated above were plotted in figure 12 normal to the expected crack profiles shown previously in figure 10(a). As seen in figure 12, in the case of θ=15 degrees, the value of $\sigma_{1'1'}$ is smaller than the shear stress whereas the two are almost equal for θ=45 degrees. For the laminates considered, the $\sigma_{1'1'}$ value near the interface appears to be highest (0.24 GPa) for θ=25 degrees.

The results discussed above indicate that the principal tension stress normal to the fiber and the shear stress parallel to the fiber near the laminate edge are highest at the interface. Therefore, the matrix crack is most likely to form in the $-\theta$ ply near the $\theta/-\theta$ interface.

5. CONCLUDING REMARKS

A $(0/\theta/-\theta)_s$ graphite epoxy laminate subjected to axial tension was analyzed using three dimensional finite element analyses. The first analysis was performed to examine the effect of matrix cracking in the -15 degree ply on the interlaminar stresses between the 15/-15 interface of a $(0/15/-15)_s$ laminate, particularly near the stress free laminate edge. Next, a strain energy release rate analysis was performed for delamination growth from a matrix crack. Then, the stress state in the uncracked laminate was analyzed to understand its effect on the crack profile in the $-\theta$ ply. Based on these analyses, the following conclusions were reached.

The interlaminar normal stress, σ_z, changed in the 15/-15 interface of a $(0/15/-15)_s$ laminate from a small compression stress when no matrix crack was present to a large tension stress near the free edge after the formation of cracking in the -15 degree ply. This indicates that the delamination from the matrix crack may initiate at the point where the matrix crack intersects the laminate edge.

For the θ=45 degree case, the strain energy release rate for a local delamination growing uniformly away from the matrix crack in the -45 degree ply is higher near the laminate edge than in the interior of the laminate.

The value of total G decreases as the delamination grows away from the matrix crack. The mode I component of G exists only near the free edge within one ply distance from the matrix crack.

The in-plane stresses in the $-\theta$ ply for the case of θ=15, and 30 degrees, in the uncracked laminate are tensile only up to a distance of 3 to 4 plies from the laminate edge along a potential crack face. The area of tension stress extends through the $-\theta$ ply thickness, to the $\theta/-\theta$ interface, only near the free edge. In contrast, the in-plane tension stress in the $-\theta$ ply for the θ=45 degree case extends across the ply thickness to the $\theta/-\theta$ interface and throughout the laminate width. This suggests that the cracking in the -45 degree ply may extend further across the laminate width.

The principal tension stress was calculated in a plane normal to the fiber direction at the laminate edge. This principal stress increased along the thickness of the $-\theta$ ply, from the center of the laminate towards the $\theta/-\theta$ interface, where it increased sharply. The shear stress acting along the fiber direction shows similar variations. Therefore, matrix cracking is likely to initiate at the free edge, near the $\theta/-\theta$ interface.

The principal tension direction is inclined at an angle to the plane of the laminate. This angle increases from the center of the laminate along the $-\theta$ ply thickness, towards the $\theta/-\theta$ interface. The projection of the matrix crack on the free edge indicates a larger curvature for smaller ply angles. This observation is consistent with the experimental findings in the literature.

To summarize, the occurrence of a high interlaminar tensile normal stress in the $\theta/-\theta$ interface due to matrix cracking in the $-\theta$ ply and the high value of

G which is localized in the vicinity of the free edge and matrix crack, will result in delamination onset in the $\theta/-\theta$ interface. The matrix cracking in the $-\theta$ ply appears to initiate at the $\theta/-\theta$ interface due to high tensile principal stress, resulting in curved crack profiles. These crack geometries must be modelled to accurately determine interlaminar stresses and G's associated with local delaminations. These solutions may then be used in progressive failure methodology for laminated composites.

6. ACKNOWLEDGEMENT

The authors would like to acknowledge the assistance provided in mesh generation by Mr. Vijay Kale of Old Dominion University.

7. REFERENCES

[1] O'Brien, T.K., Rigamonti, M., and Zanotti, C., "Tension Fatigue Analysis and Life Prediction for Composite Laminates," Int. J. of Fatigue, Vol.11, No.6, Nov. 1989, pp.379-394.

[2] O'Brien, T. K., "Towards a Damage Tolerence Philosophy for Composite Materials and Structures," Composite Materials: Testing and Design, ASTM STP 1059, American Society for Testing and Materials,Philadelphia, 1990.

[3] Soni, S.R., and Kim, R.Y., "Delamination of Composite Laminates Stimulated by Interlaminar Shear," Composite Materials:Testing and Design, Seventh Conference, ASTM STP 893, Jan.1986, pp.286-307.

[4] Lagace,P.A., and Brewer,J.C., "Studies of Delamination Growth and Final Failure under Tensile Loading," ICCM VI, London, Vol.5, Proceedings, July,1987, pp.262-273.

[5] O'Brien, T. K., and Hooper, S. J., "Fatigue Delamination Behavior of $(0_2/\theta_2/-\theta_2)_s$ Graphite Epoxy Laminates," Presented at Fourth ASTM Symposium on Composite Materials: Fatigue and Fracture, Indianapolis, Indiana, May 6-7, 1991, (NASA TM 104055).

[6] Fish,J.C., and O'Brien,T.K., "Three-Dimensional Finite Element Analysis of Delamination from Matrix Cracks in Glass-Epoxy Laminates," Composite Materials: Testing and Design, 10th Volume, ASTM STP 1120, 1992.

[7] Shivakumar, K. N., Tan, P. W., and Newman, J. C., Jr., "A Virtual Crack Closure Technique for Calculating Stress-Intensity Factors for Cracked Three-Dimensional Bodies," Int. Jnl. Fract., Vol. 36, 1988, pp. R43-R50.

[8] Salpekar,S.A., and O'Brien,T.K., "Combined Effect of Matrix Cracking and Free Edge Delamination," Composite Materials:Fatigue and Fracture, 3rd Volume, ASTM STP 1110, 1991.

[9] Groves,S.E., Harris,C.E., Highsmith, A.L., Allen, D.H., and Norvell, R.G., "An Experimental and Analytical Treatment of Matrix Cracking in Cross-Ply Laminates," EXPERIMENTAL MECHANICS, 27(1), pp.73-79, March 1987.

TABLE 1

MATERIAL PROPERTIES

AS4/3501-6 GRAPHITE EPOXY

E_{11}	= 134.45 GPa, (19.5 x 10^6 psi)
E_{22}, E_{33}	= 11.03 GPa, (1.60 x 10^6 psi)
G_{12}, G_{13}	= 5.84 GPa, (0.847 x 10^6 psi)
G_{23}	= 2.98 GPa, (0.432 x 10^6 psi)
ν_{12}, ν_{13}	= 0.301
ν_{23}	= 0.490

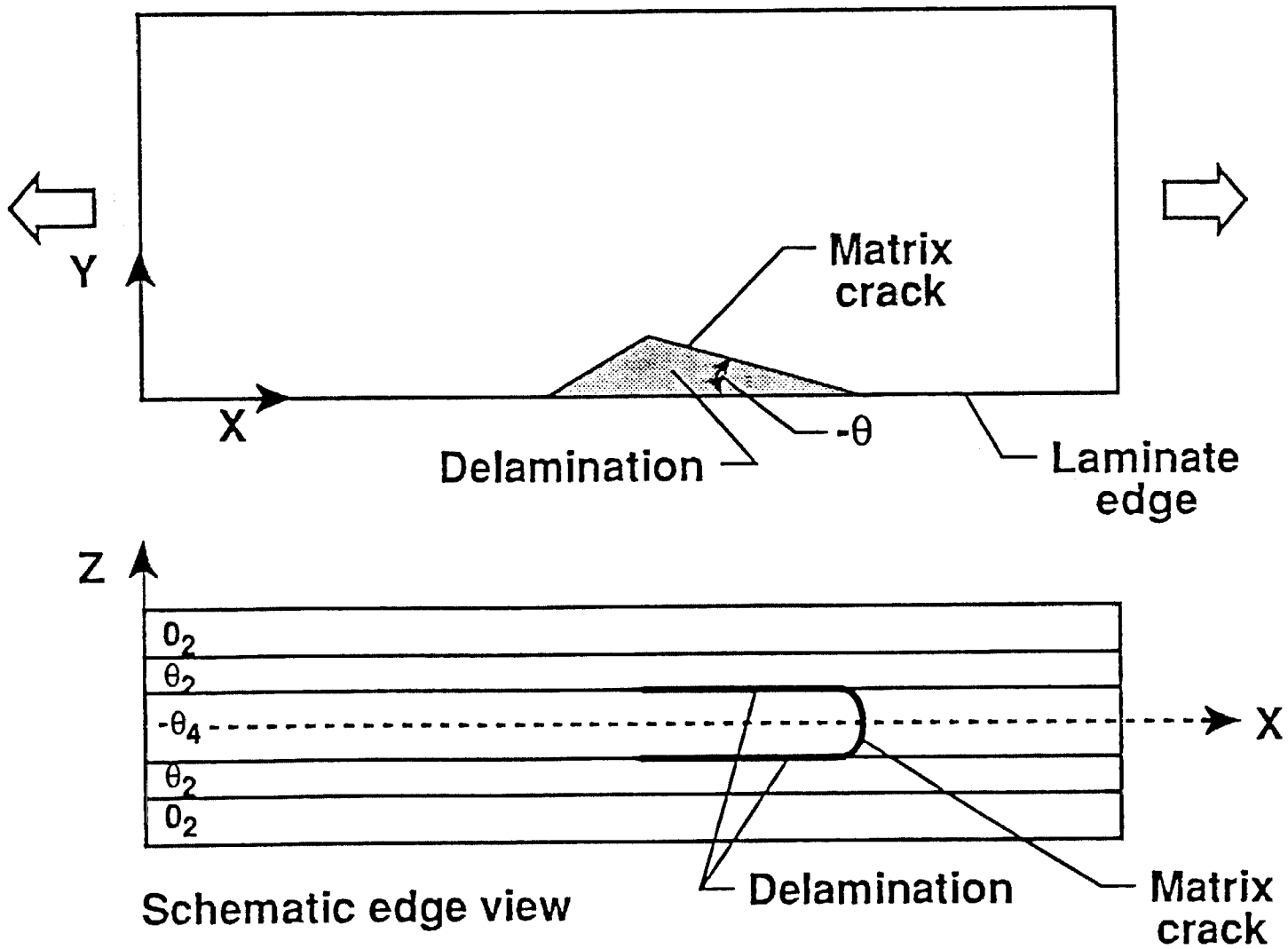

Fig. 1- Sketch of radiograph and micrograph showing delamination in $\theta/-\theta$ interface of $(0_2/\theta_2/-\theta_2)_s$ laminate (Ref. 5)

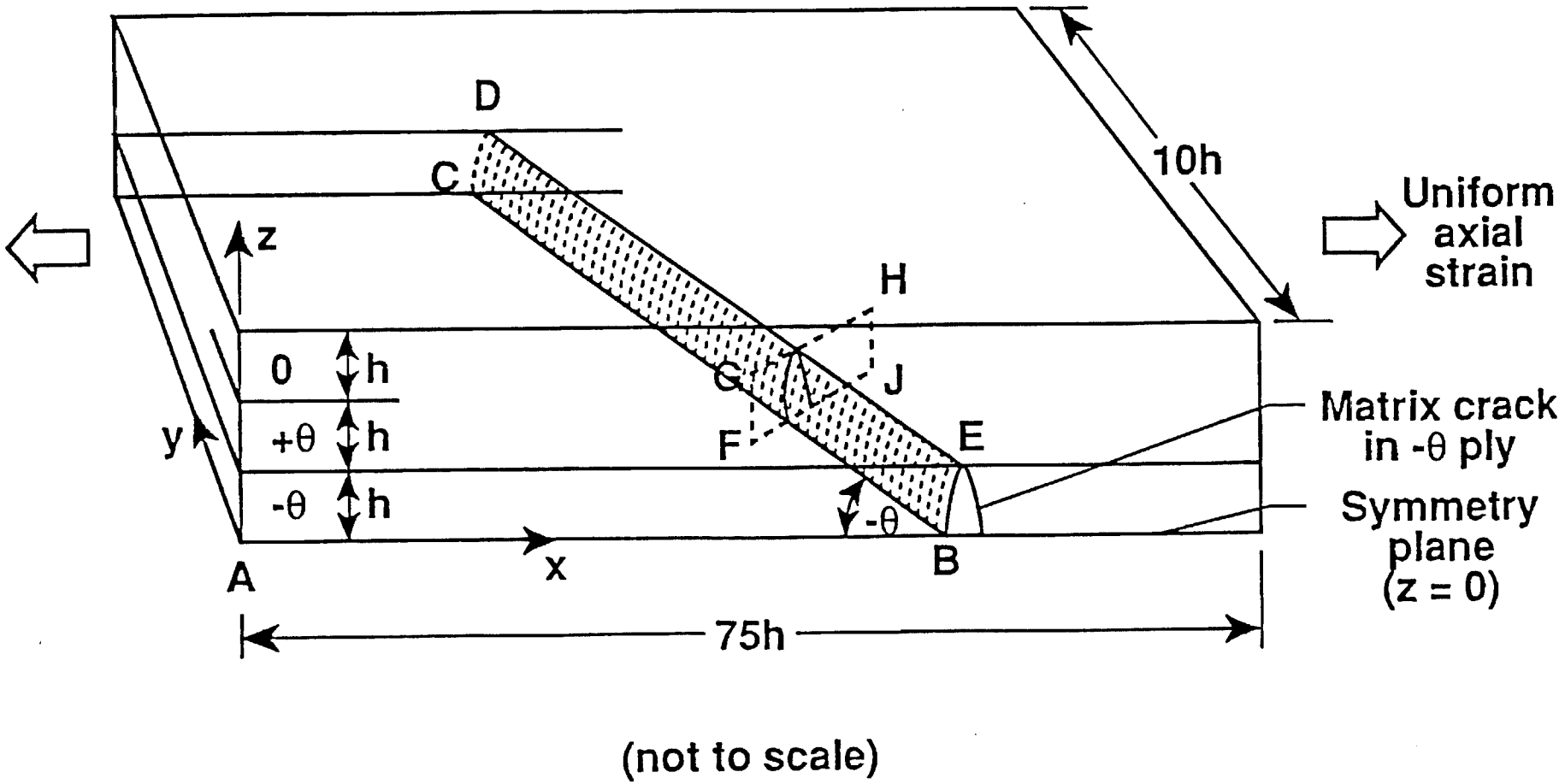

Fig. 2- Configuration and loading of a $(0/\theta/-\theta)_s$ graphite epoxy laminate

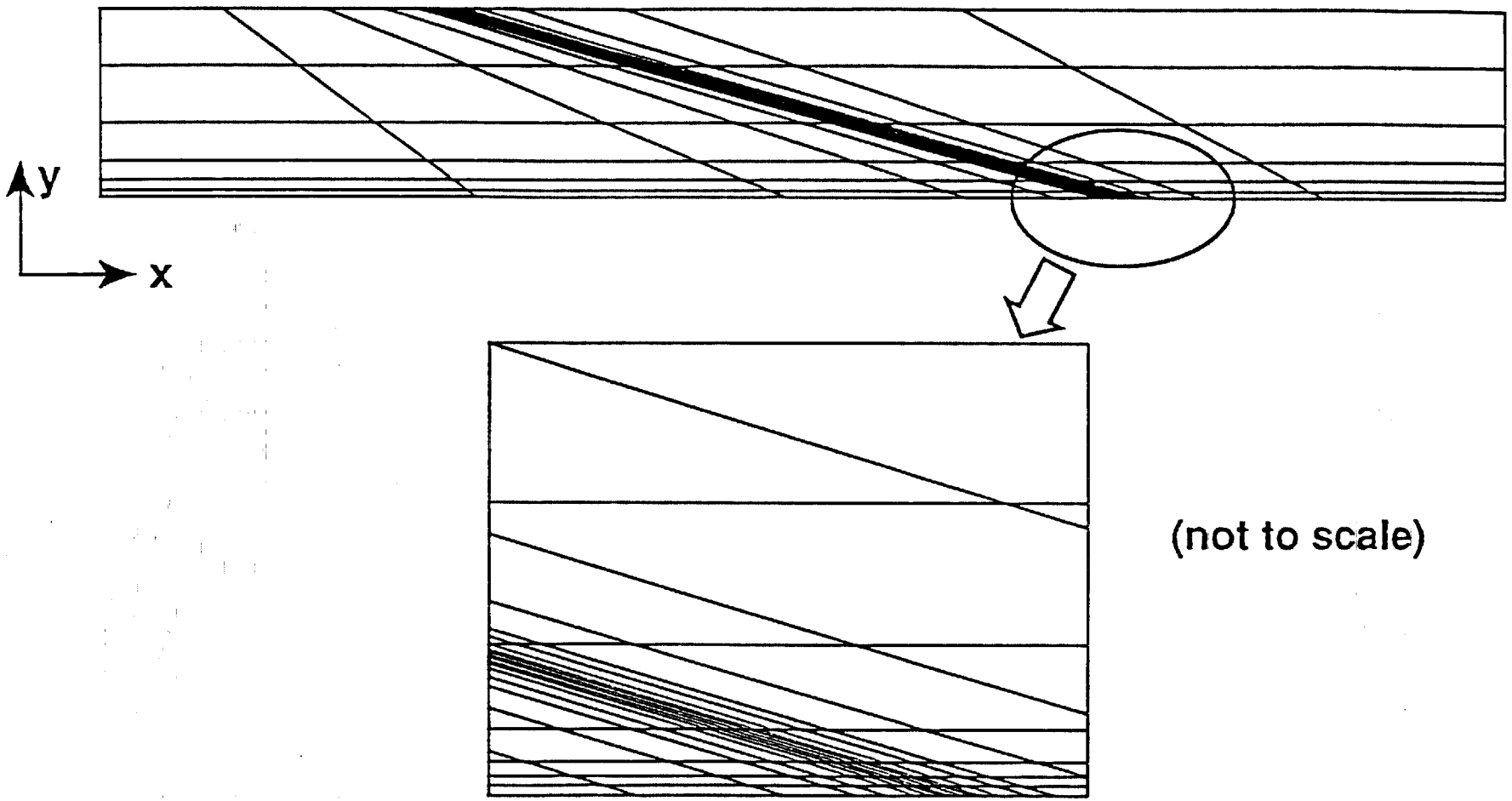

Fig. 3- View of finite element mesh in the XY plane of laminate

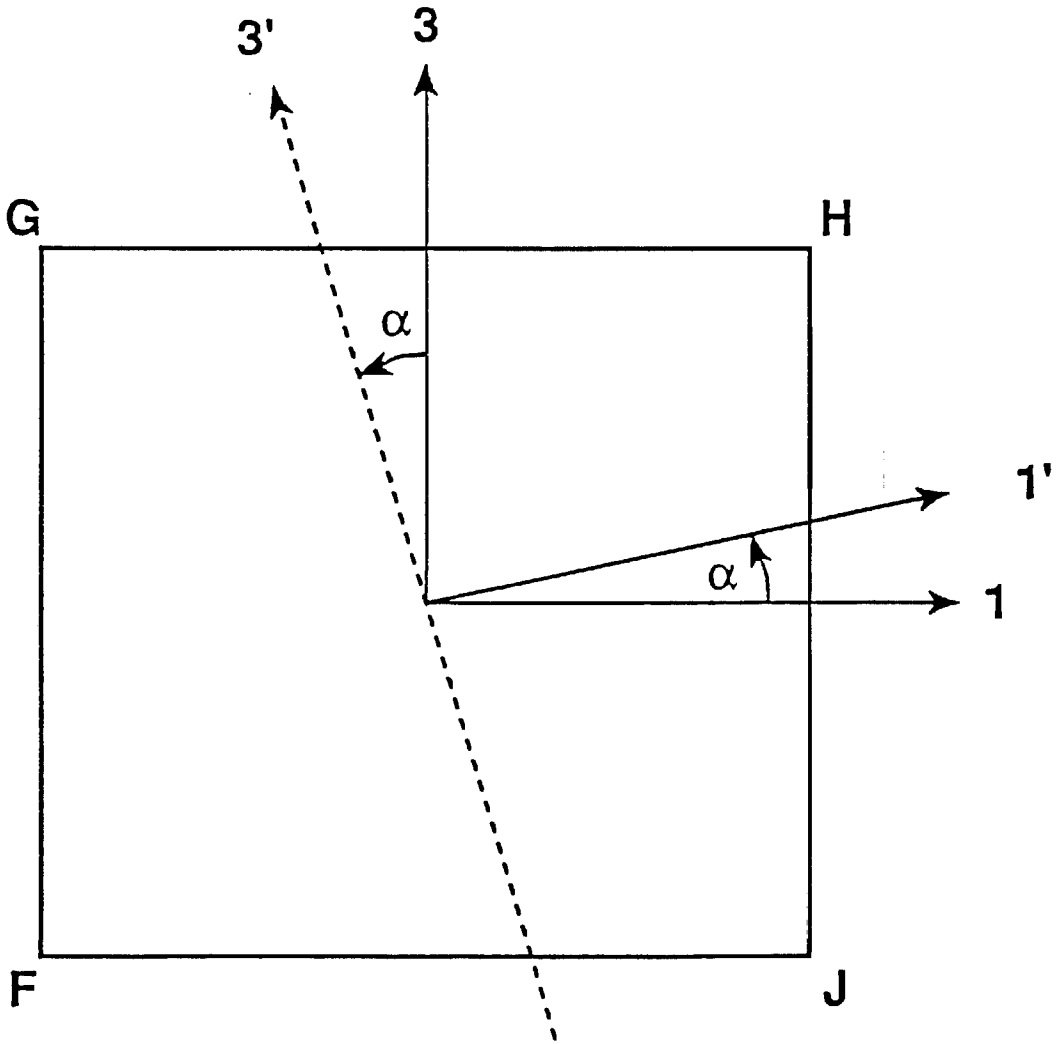

Fig. 4- Vertical section normal to matrix crack direction

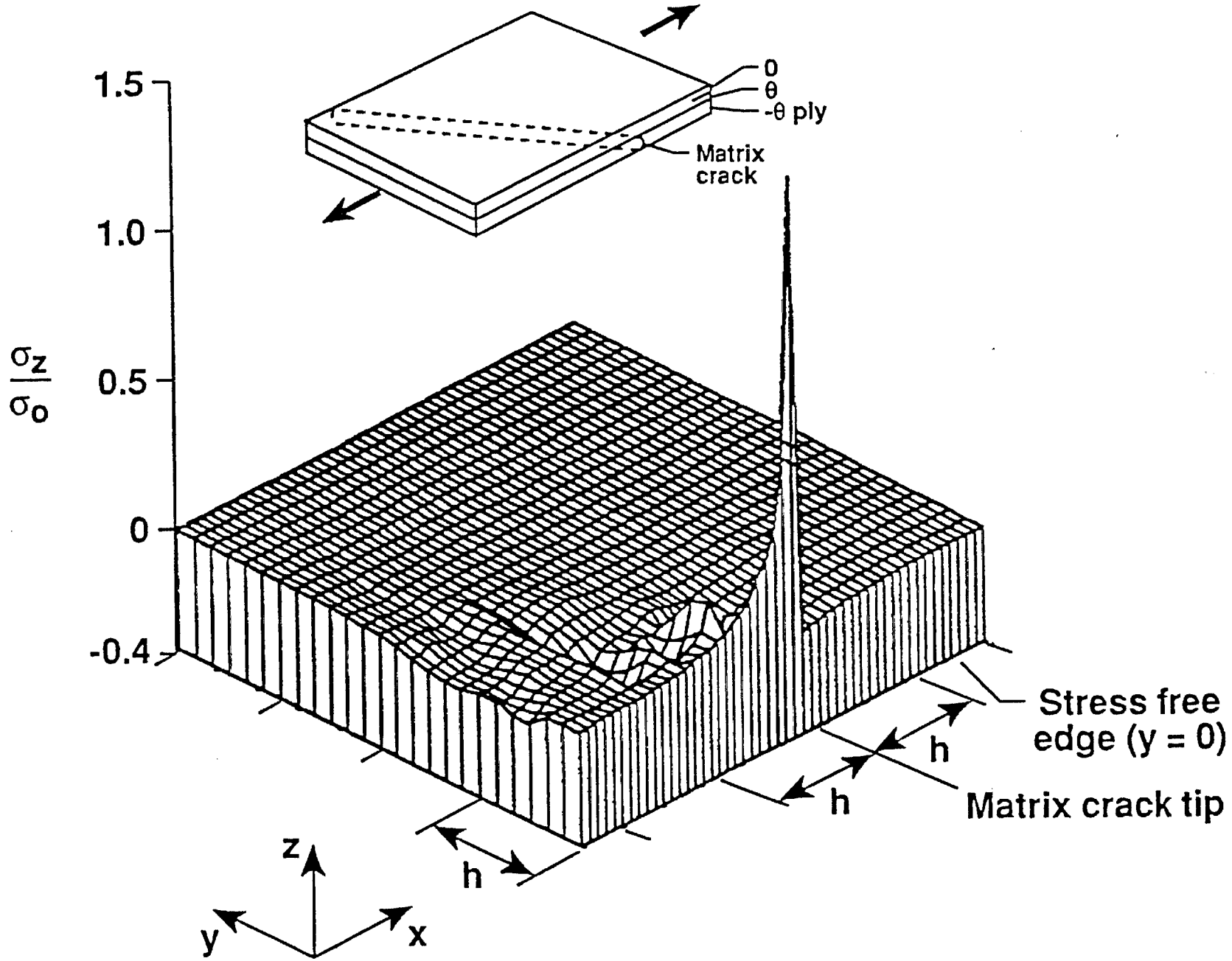

Fig. 5- Normalized interlaminar normal stress in 15/-15 interface due to matrix crack in -15 ply of $(0/15/-15)_s$ laminate

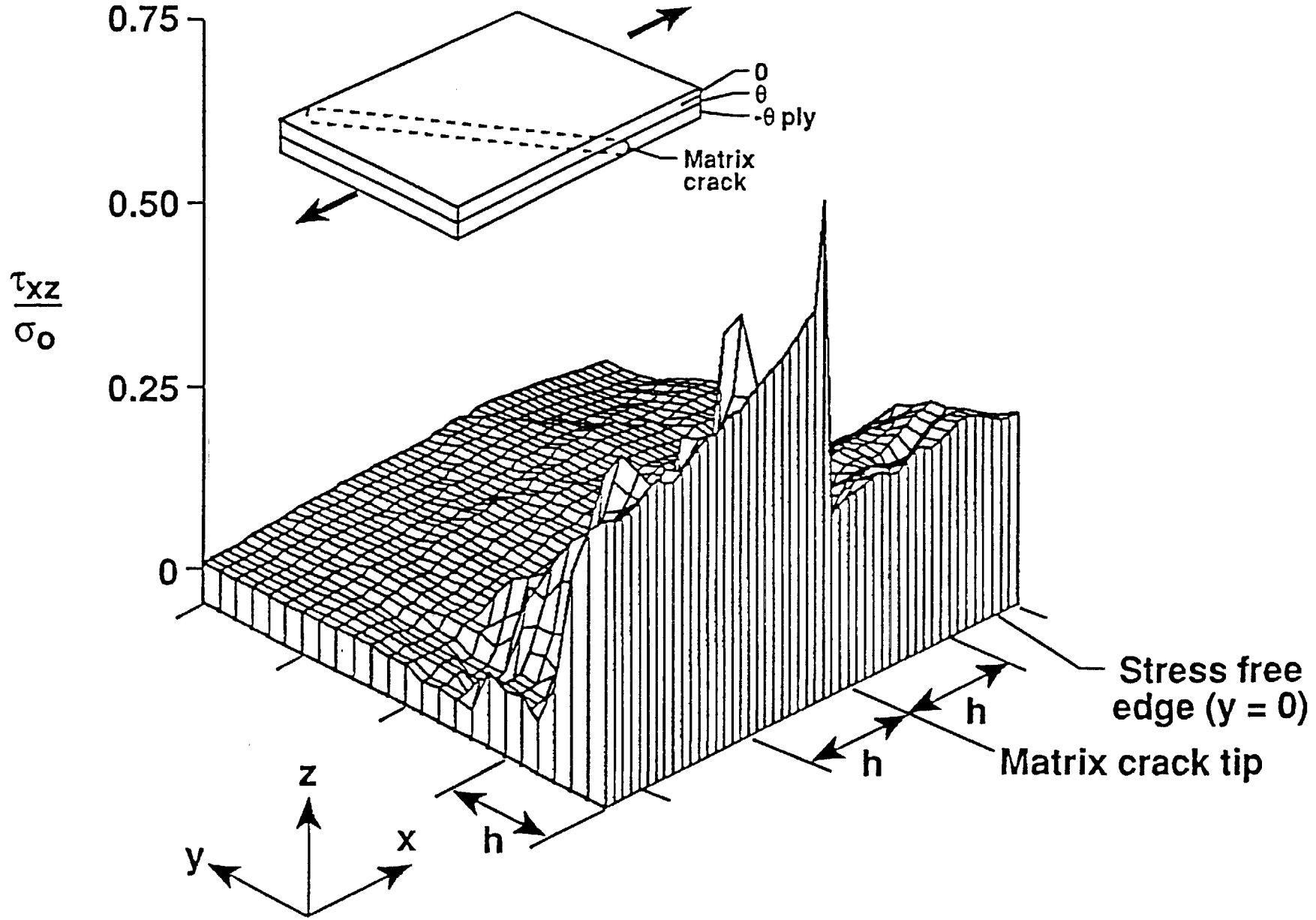

Fig. 6- Normalized interlaminar shear stress in 15/-15 interface due to matrix crack in -15 ply of $(0/15/-15)_s$ laminate

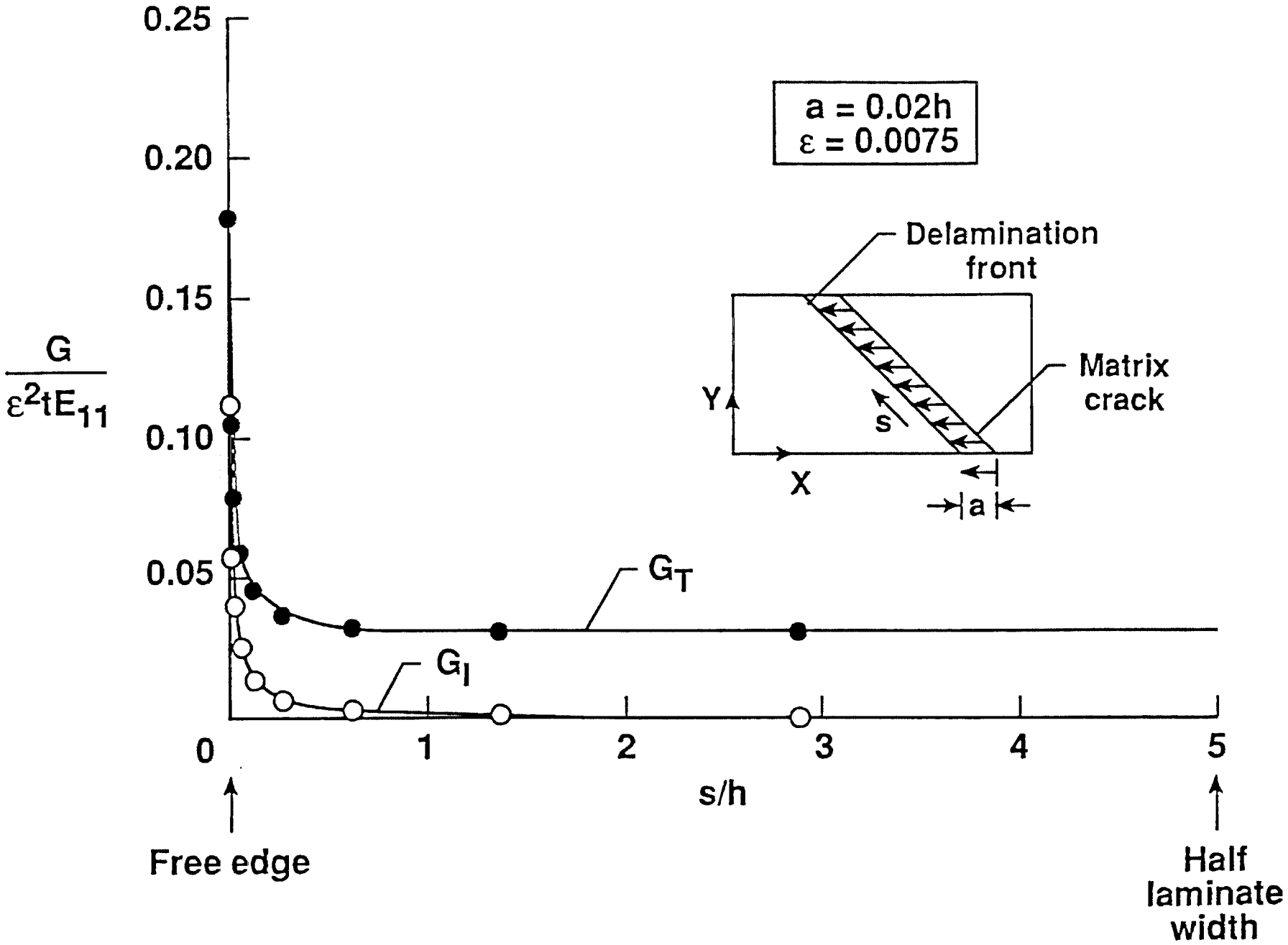

Fig. 7- Variation of G across delamination front in 45/-45 interface of $(0/45/-45)_s$ graphite epoxy laminate with a -45° ply crack

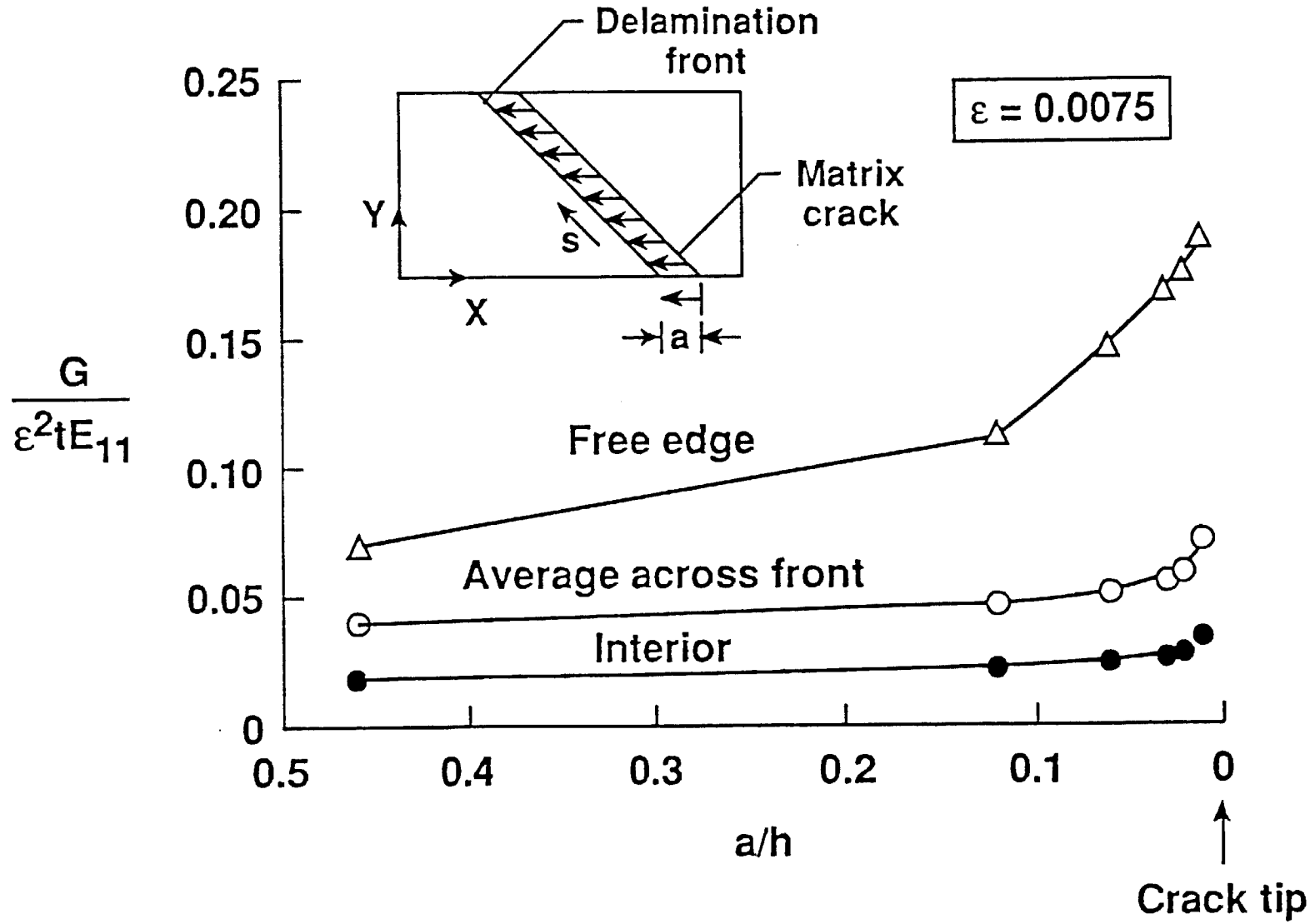

Fig. 8- Change in G due to delamination growth in $(0/45/-45)_s$ graphite epoxy laminate

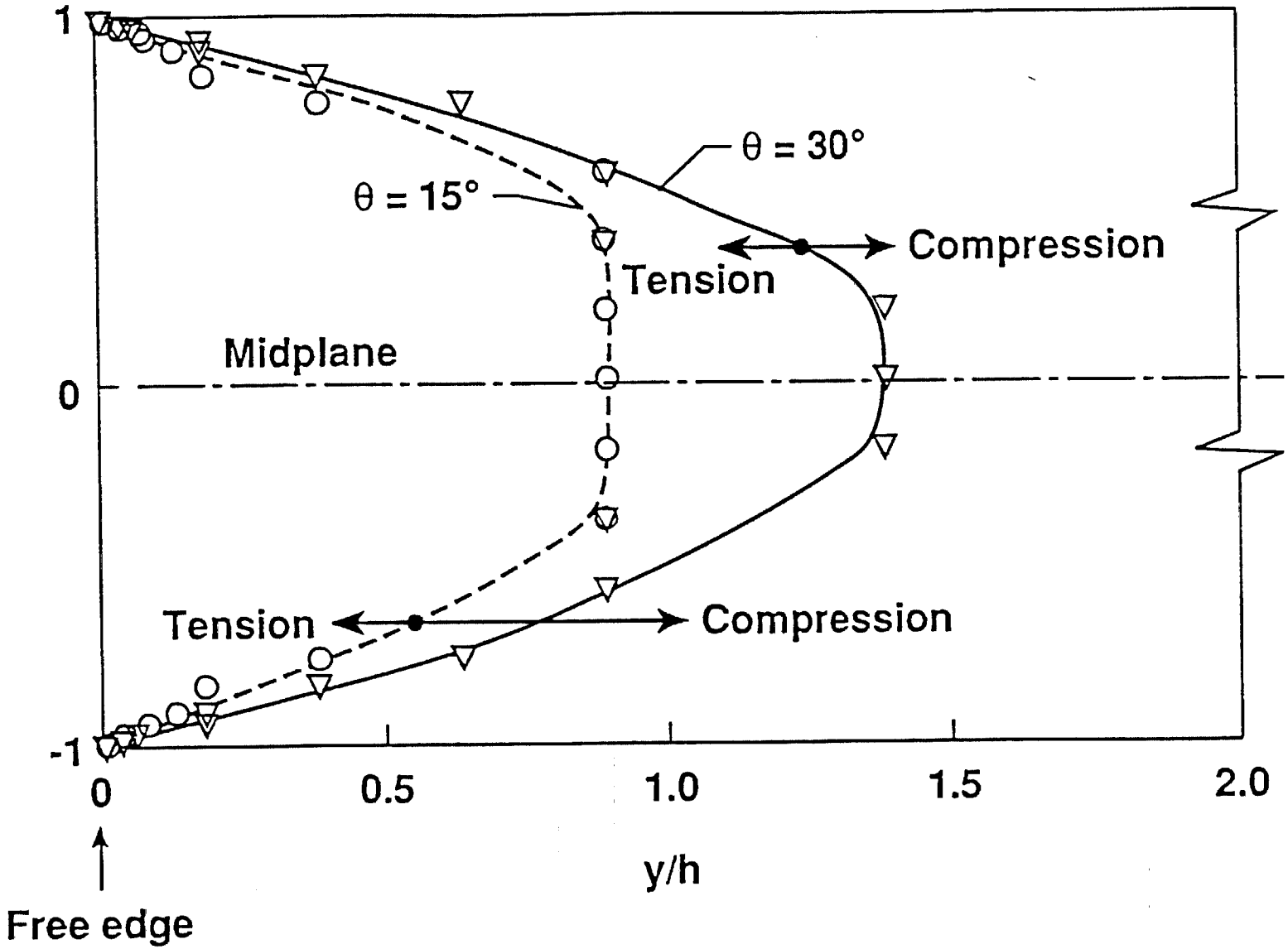

Fig. 9- Area of in-plane tension stress on a potential crack plane in the $-\theta$ ply of a $(0/\theta/-\theta)_s$ laminate

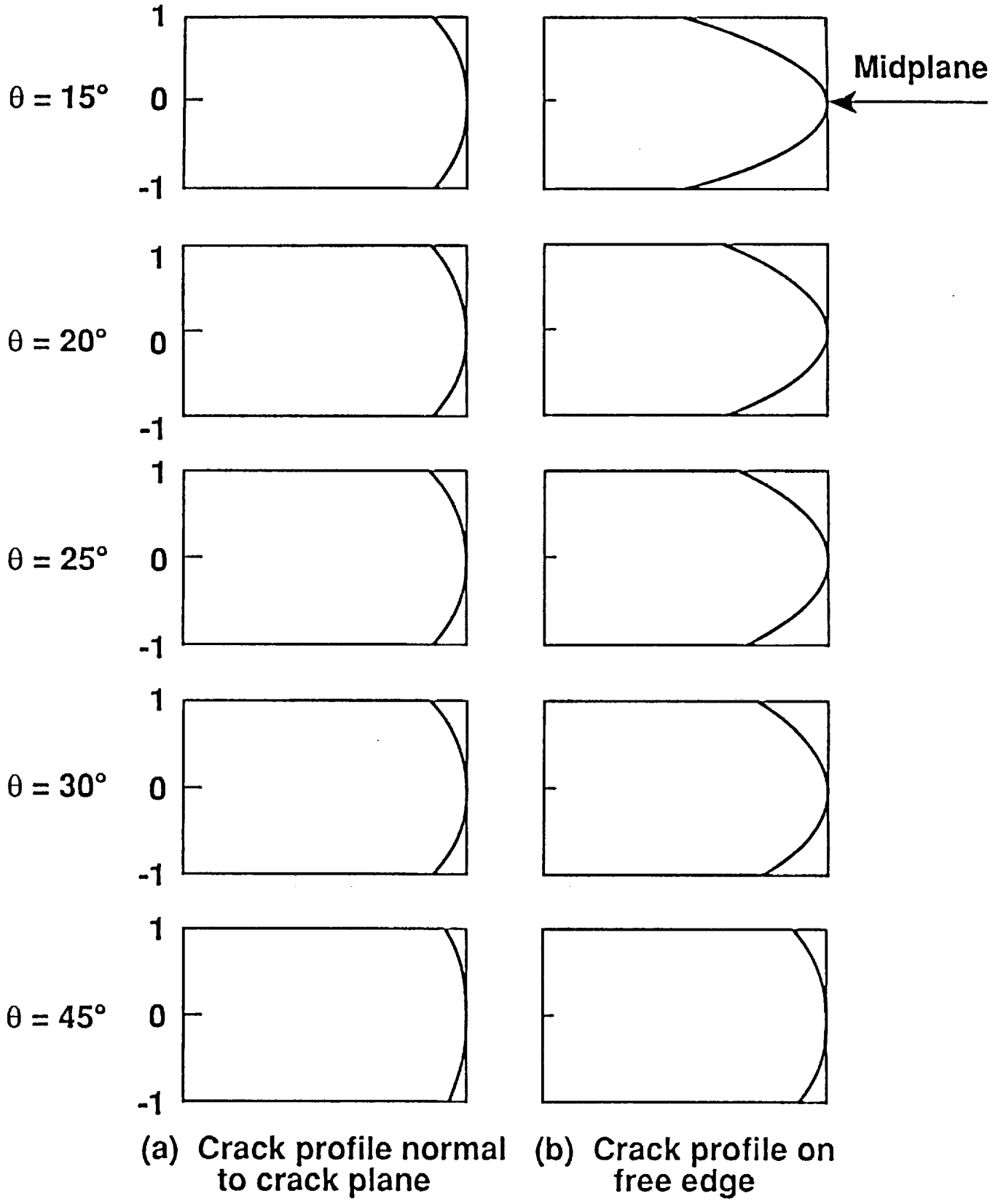

Fig. 10- Predicted crack profile in -θ plies of $(0/\theta/-\theta)_s$ laminate

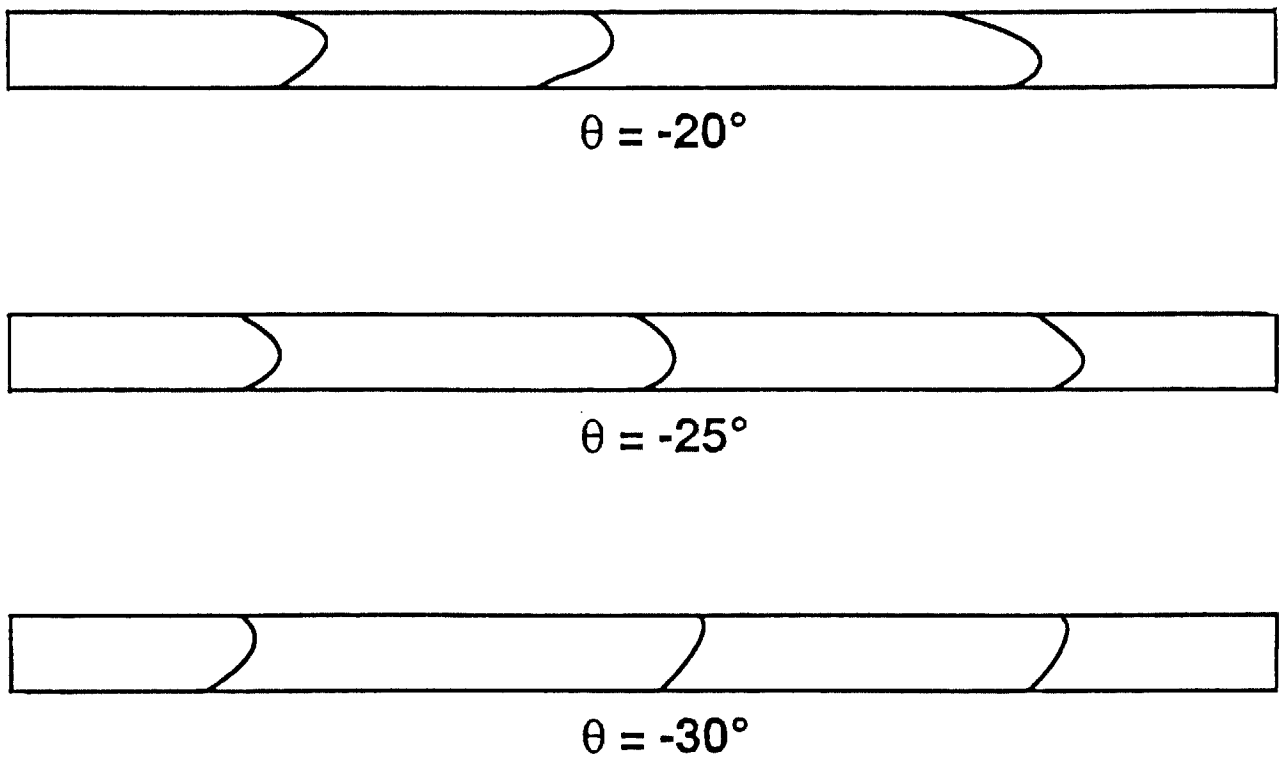

Fig. 11- Sketch of edge micrographs showing -θ matrix ply cracks in $(0_2/\theta_2/-\theta_2)_s$ laminates following cyclic loading (Ref. 5)

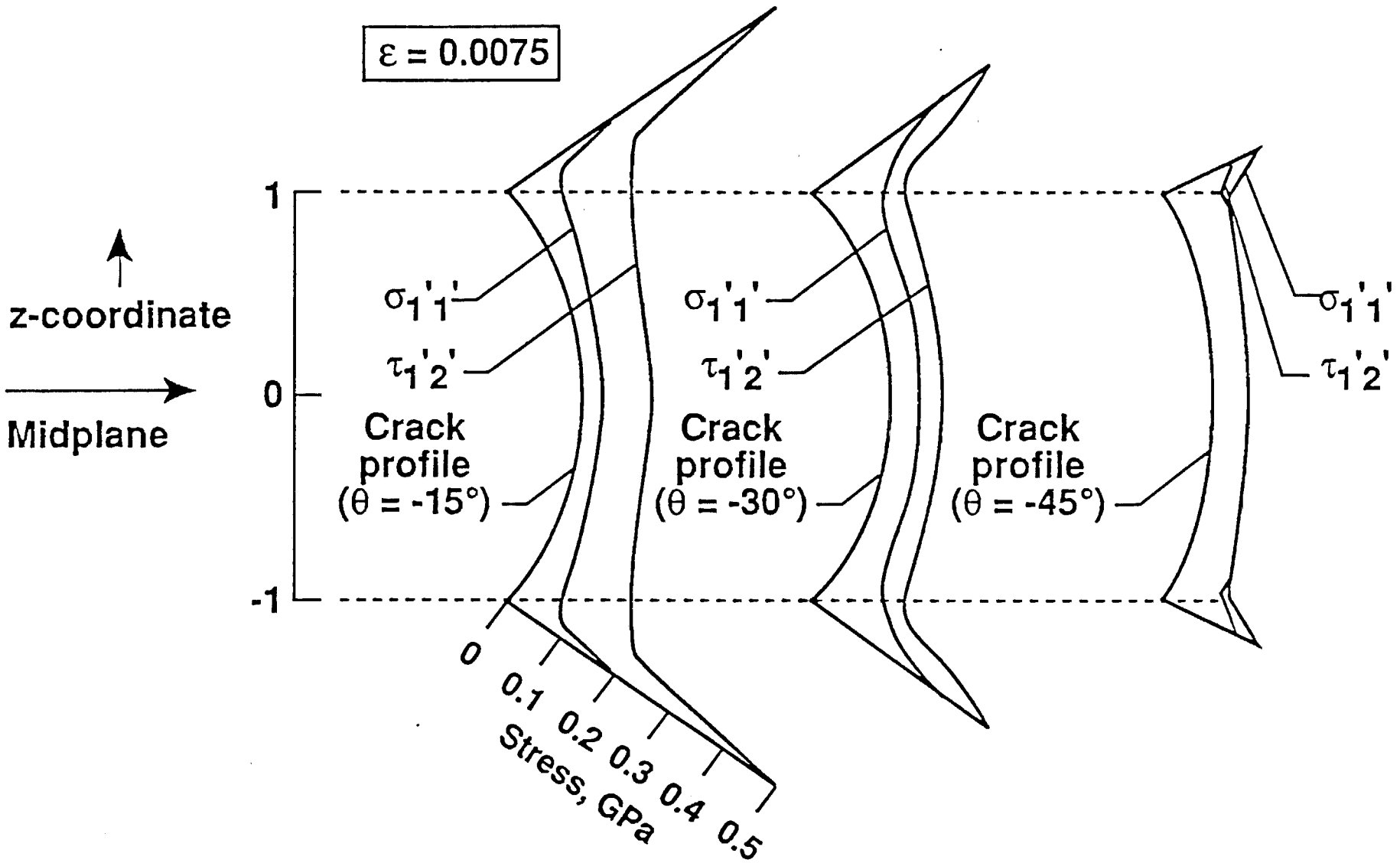

Fig. 12- Principal tension stress normal to the fiber direction and shear stress acting along the fiber direction in $-\theta^{o}$ ply of $(0/\theta/-\theta)_s$ laminates

NASA

Report Documentation Page

1. Report No.	2. Government Accession No.	3. Recipient's Catalog No.
NASA TM-104062 AVSCOM TR-91-B-002		

4. Title and Subtitle

Analysis of Matrix Cracking and Local Delamination in $(0/\theta/-\theta)_S$ Graphite Epoxy Laminates Under Tension Loading

5. Report Date	6. Performing Organization Code
March 1991	

7. Author(s)

S. A. Salpekar* and T. K. O'Brien**

8. Performing Organization Report No.	10. Work Unit No.
	505-63-01-05

9. Performing Organization Name and Address

NASA Langley Research Center, Hampton, VA 23665-5225
U.S. Army Aviation Research Technology Activity (AVSCOM)
Aerostructures Directorate
Hampton, VA 23665-5225

11. Contract or Grant No.	13. Type of Report and Period Covered
	Technical Memorandum

12. Sponsoring Agency Name and Address

National Aeronautics and Space Administration
Washington, DC 20546
U.S. Army Aviation Systems Command
St. Louis, MO 63166

14. Sponsoring Agency Code

15. Supplementary Notes

*S.A. Salpekar, Analytical Services and Materials, Inc., Hampton, VA 23666
**T. K. O'Brien, U.S. Army Aerostructures Directorate, USAARTA-AVSCOM, Langley Research Center, Hampton, VA 23665

16. Abstract

Several 3-D finite element analyses of $(0/\theta/-\theta)_S$ graphite epoxy laminates, where θ = 15, 20, 25, 30, and 45 degrees, subjected to axial tension load, were performed. The interlaminar stresses in the $\theta/-\theta$ interface were calculated with and without a matrix crack in the central $-\theta$ plies. The interlaminar normal stress changes from a small compressive stress when no matrix crack is present to a high tensile stress at the intersection of the matrix crack and the free edge. The analysis of local delamination from the $-\theta$ matrix crack indicates a high strain energy release rate and a localized mode I component near the free edge, within one ply distance from the matrix crack. In order to examine the stress state causing the matrix cracking, the maximum principal normal stress in a plane perpendicular to the fiber direction in the $-\theta$ ply was calculated in an uncracked laminate. The corresponding shear stress parallel to the fiber was also calculated. The principal normal stress at the laminate edge increases through the ply thickness and reached a very high tensile value at the $\theta/-\theta$ interface indicating that the crack in the $-\theta$ ply may initiate at the $\theta/-\theta$ interface. Crack profiles on the laminate edge in the $-\theta$ ply were constructed from the principal stress directions. The cracks were found to be more curved for layups with smaller θ angles, which is consistent with experimental observations in the literature.

17. Key Words (Suggested by Author(s))	18. Distribution Statement
Angle ply Matrix crack Delamination Three-dimensional finite element analyses Strain energy release rate	Unclassified - Unlimited Subject Category - 24

19. Security Classif. (of this report)	20. Security Classif. (of this page)	21. No. of pages	22. Price
Unclassified	Unclassified	28	A03